

# Contribution of the HMPID detector to the high- $p_T$ physics at LHC

D. Di Bari<sup>\*,†</sup>, A. Mastroserio<sup>\*,†</sup>, L. Molnar<sup>†,\*\*</sup>, E. Nappi<sup>†</sup>, D. Perrino<sup>\*,†</sup> and G. Volpe<sup>†</sup>

<sup>\*</sup>*Università degli Studi di Bari, Dipartimento Interateneo di Fisica "M. Merlin", Bari, Italy*

<sup>†</sup>*Istituto Nazionale di Fisica Nucleare, Sezione di Bari, Italy*

<sup>\*\*</sup>*Res. Inst. Particle & Nucl. Phys., Hungarian Academy of Sciences, Hungary*<sup>1</sup>

**Abstract.** The LHC will deliver unexplored energy regimes for proton-proton and heavy-ion collisions. As shown by the RHIC experiments, particle identification over a large momentum range is essential to disentangle physics processes, especially in the intermediate  $p_T$  ( $1 < p_T < 5$  GeV/c) region. The novel design of the High-Momentum Particle Identification Detector (HMPID), based on large surface CsI photocathodes, is able to identify  $\pi^\pm$ ,  $K^\pm$ ,  $p$  and  $\bar{p}$  in the momentum region where bulk medium properties and hard scatterings interplay. Furthermore, measurement of resonance particles such as the  $\phi \rightarrow K^+K^-$  could provide information on the system evolution. The HMPID layout and segmentation are optimized to study particle correlations at high momenta describing the early phase and the dynamical evolution of the collision. At LHC, the increased hard cross section will significantly be enhanced compared to RHIC. Jet reconstruction via Deterministic Annealing can address jet quenching and detailed measurements of jet properties. In this paper, we present these selected topics from the possible HMPID contributions to the physics goals of LHC.

**Keywords:** LHC, HMPID, heavy-ion, Ring Imaging Cherenkov Detector.

**PACS:** 25.75.-q,25.75.Ag,29.40.Ka

## THE HIGH-MOMENTUM PARTICLE IDENTIFICATION DETECTOR

The High Momentum Particle Identification Detector (HMPID) [1], consists of seven identical Ring-Imaging Cherenkov modules, covering 11 m<sup>2</sup> in total in a single arm arrangement. The HMPID exploits the properties of Cherenkov light production and large surface CsI photocathodes to identify charged particles on track-by-track basis. Charged particles traversing the detector produce Cherenkov photons in the C<sub>6</sub>F<sub>14</sub> radiator ( $\langle n \rangle \approx 1.292$ ). The Cherenkov photons are detected by MWPCs. One photocathode of the MWPC is the segmented CsI photocathode where the typical ring pattern is formed. A dedicated algorithm of pattern recognition gives information on the mean Cherenkov photon emission angle ( $\Theta_C$ ). Hence, the HMPID can identify charged pions and kaons in the momentum range  $p \sim 1 - 3$  GeV/c and protons up to  $p \sim 5$  GeV/c with  $3\sigma$  separation. Detailed description of the HMPID can be found in [1].

---

<sup>1</sup> This work was partially supported by the grants OTKA NK62044, IN71374.

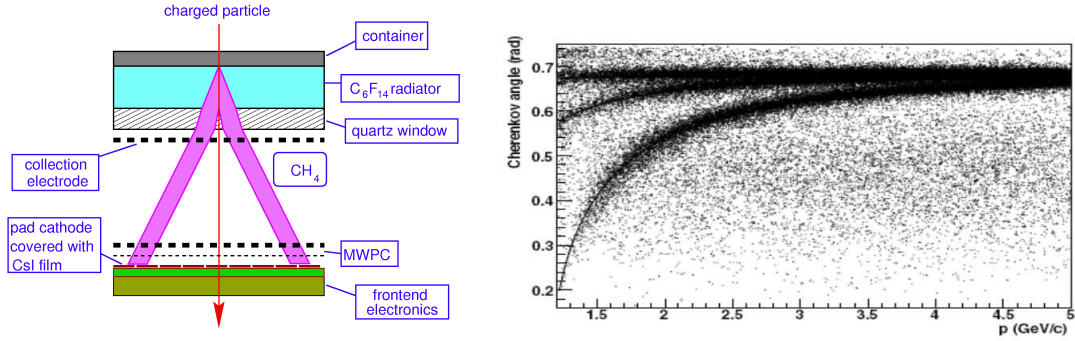


**FIGURE 1.** Left: Schematic view of the HMPID [1]. Right: Reconstructed Cherenkov angle in the HMPID as a function of the track momentum. Equal concentration of charged pions, kaons and protons have been merged with HIJING events ( $dN_{\text{ch}}/d\eta = 6000$ ). Solid lines indicate the predicted curves for  $\pi$ ,  $K$  and  $p$  [2].

## HMPID RELATED OBSERVABLES: SINGLE HADRON SPECTRA AND $\Phi(1020)$

Some signals of the Quark Gluon Plasma (QGP) are influenced by the mechanisms involved at the hadronization stage [3], therefore it is important to disentangle such effects from the deconfined state observables. The momentum region between 2 and 5 GeV/c is crucial to this aim. At the Relativistic Heavy Ion Collider (RHIC), where Au nuclei were collided at  $\sqrt{s_{NN}} = 200$  GeV, hadron production seems to be driven by quark content dependent mechanisms. A striking result is that the baryon over meson ratio reaches unity in most central collisions and the mechanism of the quark coalescence at the hadronization describes quite well such a behavior [3]. The left and the central panel in Figure 2 show the unexpected deviation of such a ratio from p-p events where the deconfined state is not expected to form. Furthermore, the elliptic flow of the expanding fireball reaches different values depending on the quark content of the hadrons (right panel in Figure 2). Within this scenario the  $\phi(1020)$  has a meson nature ( $s\bar{s}$  bound state) and a proton-like mass, therefore it is a good tool to probe the QGP and the role of both mass values and quark content in its subsequent hadronization phase. Strange quarks are mainly produced by gluon fragmentation within the hot and dense medium, therefore the short lifetime of  $\phi$  and its small cross section with non strange hadrons [4] make this particle a good tool to probe both the deconfined and the newly formed hot hadronic state. An interesting result is the elliptic flow of  $\phi$ : it follows a mass ordering, falling between the heavier  $\Lambda$  and the  $K^0$ , up to 2 GeV/c and then it follows the  $K^0$  trend [5]. These measurements suggest that a comparison between the  $\phi(1020)$  and the proton production can provide new insights on the effects of both QGP and the first hot confined state and the HMPID detector can identify  $\phi$  mesons and protons right between 2 and 5 GeV/c (Left plot in Figure 3).

Furthermore, recent theoretical results of hadron momentum distribution at LHC energies show that between 2 and 5 GeV/c the predictions from hydrodynamical estimates for protons do not match smoothly to the respective pQCD + partonic energy loss cal-

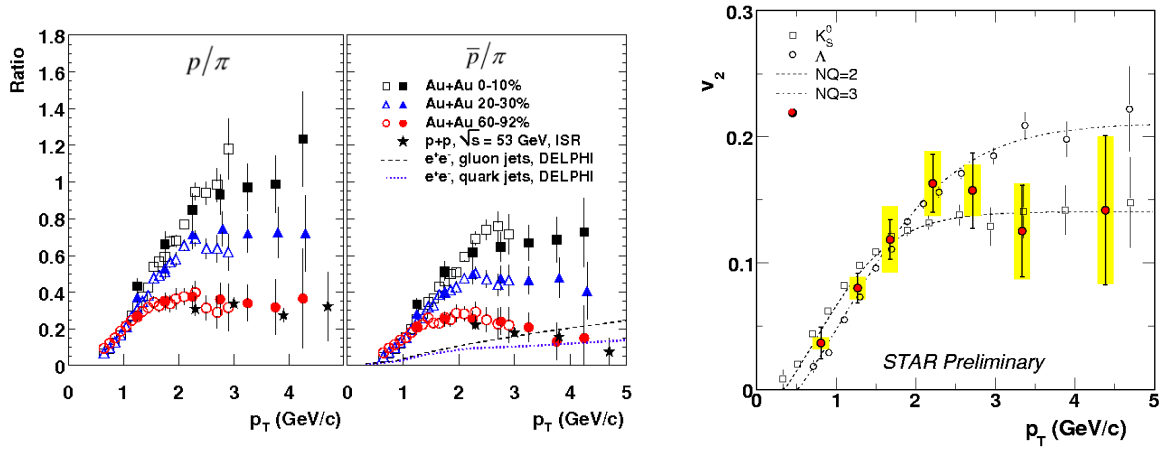


**FIGURE 2.** Left: The  $p/\pi$  ratios are shown for different centralities in 200 GeV Au-Au collisions. The ratio reaches 1 in the most central collisions. A comparison with p-p collisions is also shown [6]. Right:  $\phi(1020)$  elliptic flow (filled circles) is shown with respect to the  $\Lambda$  and the  $K^0$ . The  $v_2$  follows the baryon trend up to 2 GeV/c, then it behaves like the  $K^0$  [5].

culations, within the uncertainty bands. This implies that future measurements of the proton momentum distribution itself within this peculiar momentum region will be very important to understand the dynamics of heavy-ion collisions.

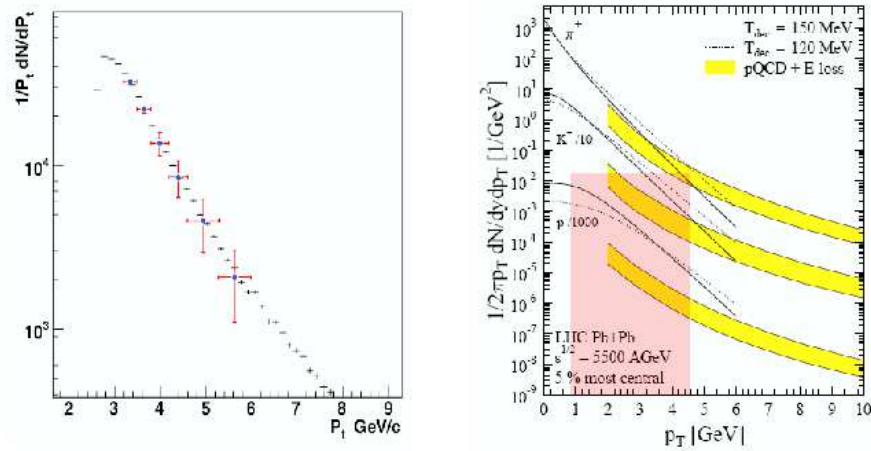


**FIGURE 3.** Left: Reconstructed momentum spectrum of the  $\phi(1020)$  meson in its hadronic decay channel  $\phi \rightarrow K^+K^-$  in central Pb-Pb collisions at 5.5 TeV by simulation. The kaons were identified by the HMPID between  $p_T \approx 1.3 - 6$  GeV/c. Right: Predictions for  $\pi$ ,  $K$  and  $p$  momentum distributions at LHC energies [7]. For protons there is no continuity between hydrodynamical curve and pQCD+energy loss results between 2 and 5 GeV/c, the region where the HMPID can identify them.

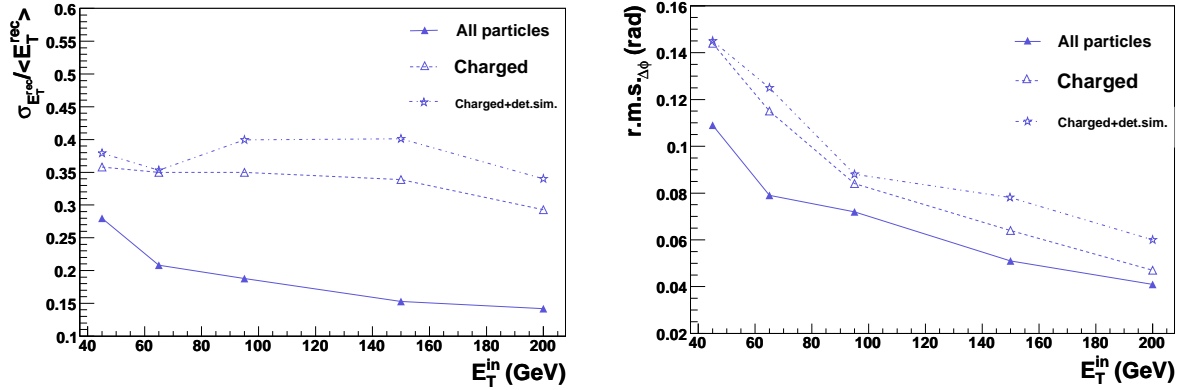


**FIGURE 4.** Left: Energy resolution of reconstructed jets as a function of different generated jet energy, when all particles (full line), charged particles (dashed line) are considered, and with fast detector response simulation (dotted line). Right: Direction resolution of reconstructed jets as a function of different generated jet energy.

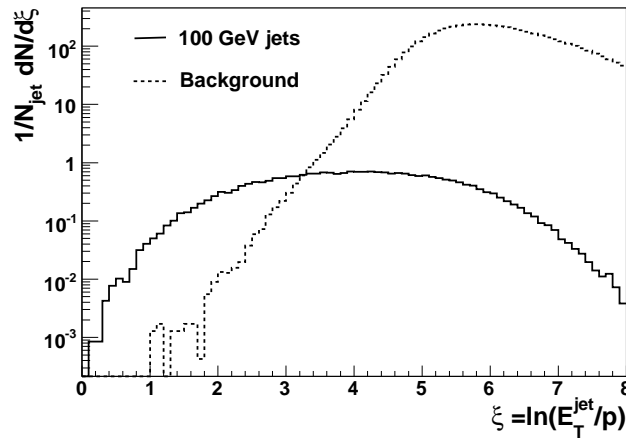


**FIGURE 5.** Fragmentation function for 100 GeV PYTHIA jets reconstructed with DA, compared with background coming from central Pb-Pb (HIJING) collisions.

## DETERMINISTIC ANNEALING

At LHC, the 98% of total cross section will be represented by hard processes. For this reason, jet production will be copious and jet studies will be suitable to probe the hot and dense matter that will be formed in heavy-ion collisions. A new algorithm, Deterministic Annealing (DA), has been recently developed for jet finding in ALICE. It satisfies important theoretical and experimental requirements [8] and it has been tested on simulated p-p and Pb-Pb collisions. Results from the DA algorithm are shown in Figure 4, obtained from simulated PYTHIA jet events embedded into Pb-Pb HIJING events, both generated at  $\sqrt{s_{NN}} = 5.5$  TeV. The transverse energy and the direction resolution of the reconstructed jets as a function of  $E_T^{\text{in}}$  is referred to the same monochromatic input spec-

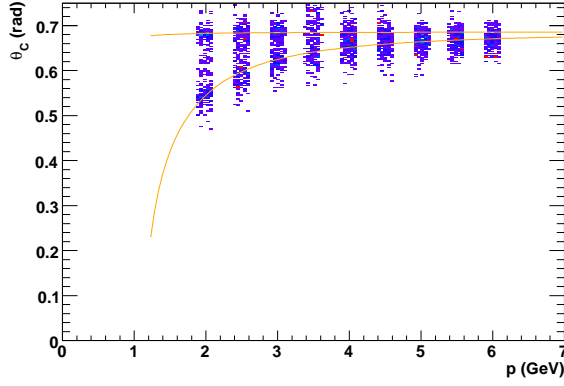


**FIGURE 6.** Studied momentum regions are shown with the extracted  $\Theta_C$  for particle identification.

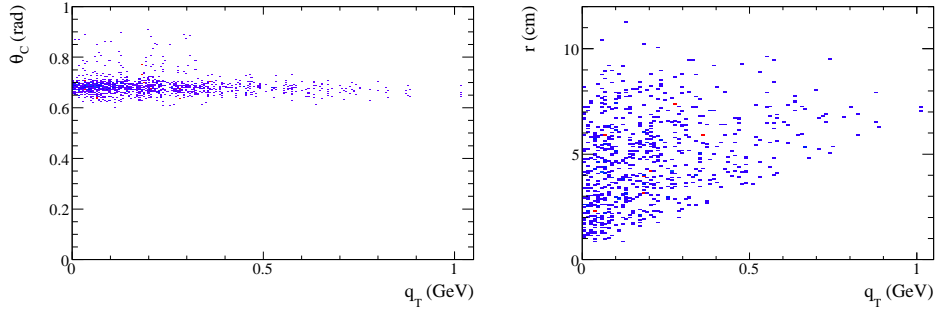


**FIGURE 7.**  $\Theta_C$  and distance of MIPS (tracks) as a function of  $q_T$  variables are shown.

trum of jets, reconstructed with the DA algorithm in a background free environment. While for ideal response detectors analysis (i.e. considering all the particles) energy resolution always improves with energy, charged-to-neutral fluctuations dominate when ALICE reconstruction capabilities are considered. It can be noticed that, even with fast simulation, energy resolution reaches at most 40%, a value that is similar to the one achieved by cone algorithm with a small radius [9]. As regards direction resolution, it smoothly improves as the input jets transverse energy grows, as one could expect.

HMPID will contribute to the study of jet properties. In fact, the influence of medium on parton propagation after the hard scattering can be studied comparing the leading particle fragmentation between p-p and Pb-Pb collisions. In particular, from PYTHIA jet quenching simulation an enhancement of this function in the low  $p_T$  region, and a corresponding depletion in the lower  $\xi$  values region, more visible for higher values of the transport coefficient  $\langle \hat{q} \rangle$ , can be observed [2]. In Figure 5 the fragmentation of jets found with Deterministic Annealing is compared with background particles included in the same jet surface, coming from Pb-Pb collisions. As a practical example, for 100 GeV jets  $\xi \approx 3.5$  corresponds to  $p \approx 3$  GeV/c, that is inside the HMPID  $p_T$  coverage.

## HBT FEASIBILITY STUDY

This final-state information of heavy-ion collisions is more directly accessed by interferometric methods, such as the Hanbury-Brown and Twiss (HBT) measurement. At LHC, due to the high multiplicity, event-by-event HBT could be performed. To achieve event-by-event HBT measurements,  $3\sigma$  separation in particle identification [2] is required. The HMPID can contribute in the high- $p_T$  region: to  $\pi^\pm\pi^\pm$ ,  $K^\pm K^\pm$  and  $p^\pm p^\pm$  HBT measurements. Furthermore, non-identical correlations, such as  $p$ - $\Lambda$  could be performed to investigate the contribution of flow effects. A preliminary study on the HMPID detector resolution of two close tracks addresses the capabilities of HMPID for HBT. Fast MC simulations of two tracks ( $\pi$ - $\pi$  and  $p$ - $p$ ) in close phase space (at least one pad separation) and in various momentum bins are performed, including complete simulation of HMPID response in a 0.2 T magnetic field. The extracted  $\Theta_C$  as a function of the studied momentum regions is shown in Figure 6 for charged pions and protons. Figure 7 shows the  $\Theta_C$  for charged pions and the extracted distance of two tracks for protons as a function of  $q_T$ . Resolution down to  $q_T \sim 10 - 50$  MeV is achievable with the default pattern recognition algorithm.

## SUMMARY

RHIC results have shown that QCD alone is not enough to describe the full spectrum of hadronic physics in ultrarelativistic heavy-ion collisions. Especially in the momentum range 2 - 5 GeV/ $c$ , where both hard and soft processes come into play. Measurements in this region could give insights to the processes that drive the collision evolution. At LHC energies the High Momentum Particle Identification detector will identify charged pions, kaon and protons and also resonances such as  $\phi(1020)$  in the above momentum region. Details of the HMPID design and its working principles were shortly presented. Furthermore, selected physics topics of the HMPID were discussed such as jet reconstruction via Deterministic Annealing and particle correlations.

## REFERENCES

1. CERN / LHCC 98 - 19 ALICE TDR 1998.
2. B. Alessandro *et al.* [ALICE Collaboration], J. Phys. G **32**, 1295 (2006).
3. V. Greco and C. M. Ko, Acta Phys. Hung. A **24**, 235 (2005) [arXiv:nucl-th/0405040], B. I. Abelev *et al.* [STAR Collaboration], Phys. Rev. Lett. **97**, 152301 (2006) [arXiv:nucl-ex/0606003].
4. A. Shor, Phys. Rev. Lett. **54** (1985) 1122.
5. B. I. Abelev *et al.* [STAR Collaboration], Phys. Rev. Lett. **99**, 112301 (2007) [arXiv:nucl-ex/0703033].
6. S. S. Adler *et al.* [PHENIX Collaboration], Phys. Rev. Lett. **91**, 172301 (2003) [arXiv:nucl-ex/0305036].
7. K. J. Eskola, H. Honkanen, H. Niemi, P. V. Ruuskanen and S. S. Rasanen, Phys. Rev. C **72**, 044904 (2005) [arXiv:hep-ph/0506049].
8. G. C. Blazey *et al.*, arXiv:hep-ex/0005012.
9. S. L. Blyth *et al.*, J. Phys. G **34**, 271 (2007) [arXiv:nucl-ex/0609023].